Exp Fluids (2010) 49:1219–1229
DOI 10.1007/s00348-010-0866-4

RESEARCH ARTICLE

Perpendicular ultrasound velocity measurement by 2D cross correlation of RF data. Part B: volume flow estimation in curved vessels

Bart Beulen · Anna Catharina Verkaik · Nathalie Bijnens · Marcel Rutten · Frans van de Vosse

Received: 1 August 2009 / Revised: 2 March 2010 / Accepted: 15 March 2010 / Published online: 2 April 2010

Abstract A novel axial velocity profile integration method, obtained from ultrasonic perpendicular velocimetry, for flow estimation in curved tubes was validated. In an experimental set-up, physiologically relevant curved geometries and flows were considered. Axial velocity profile measurements were taken by applying particle imaging velocimetry-based methods to ultrasound data acquired by means of a linear array transducer positioned perpendicular to the axial velocity component. Comparison of the assessed asymmetric velocity profiles to computational fluid dynamics calculations showed excellent agreement. Subsequently, the recently introduced cos θ-integration method for flow estimation was compared to the presently applied Poiseuille and Womersley models. The average deviation between the cos θ-integration-based unsteady flow estimate and the reference flow was about 5%, compared to an average deviation of 20% for both the Poiseuille and Womersley approximation. Additionally, the effect of off-centre measurement was analysed for the three models. It was found that only for the cos θ-integration method, an accurate flow estimation is feasible, even when it is measured off centre.

1 Introduction

Haemodynamic factors play a significant role in the development and localization of cardiovascular disease (CVD; Fung 1993; Caro et al. 1971). Arteries affected by CVD in general show thickening and stiffening of the vessel walls, leading to elevated blood pressure (Laurent et al. 2006). To deduce the biomechanical parameters that are related to the development of CVD, such as compliance, wall shear stress, pulse wave velocity and vascular impedance, and to obtain local hemodynamic variables, the pressure and flow at specific areas of the arterial system need to be monitored, by preference non-invasively and simultaneously.

In clinical practice, ultrasound is frequently used as a non-invasive method to obtain geometric and haemodynamic variables such as blood (centreline) velocity, wall shear stress, vessel diameter, intima-media thickness (IMT) and pulse wave velocity (PWV; Brands et al. 1998, 1999). The local flow is derived from the vessel diameter and blood velocity assessment. Currently, often Doppler ultrasound is applied to perform velocity measurements. The ultrasound probe needs to be positioned at a certain insonification angle (non-perpendicular) with respect to the blood velocity vector. A reliable velocity assessment necessitates this angle to be accurately known and constant during the measurement. Deviations in insonification angle result in velocity errors of the same order (Fillinger and Schwartz 1993; Gill 1985). For flow estimation, a certain velocity distribution, e.g., a Poiseuile or Womersley profile is assumed, and the flow is calculated based on the maximum or centreline velocity (Douchette et al. 1992). The Poiseuille approximation is suitable for quasi-static flow in straight arteries, whereas the Womersley approximation is valid for in-stationary flow in straight arteries. However, most arteries are tapered, curved and bifurcating, causing the axial velocity distribution to be altered by transversal velocities, resulting in asymmetrical axial velocity profiles and consequently in inaccurate flow estimations (Krams

B. Beulen · A. C. Verkaik · N. Bijnens (✉) · M. Rutten · F. van de Vosse
Section Cardiovascular Biomechanics,
Department of Biomedical Engineering,
Eindhoven University of Technology,
PO Box 513, 5600 MB Eindhoven, Netherlands
e-mail: n.bijnens@tue.nl

et al. 2005). Additionally, the position of the vessel walls needs to be known exactly in order to perform the integration of velocity to flow. An accurate assessment of the wall position is only achievable with the ultrasound beam positioned perpendicular to the vessel. As a result, a simultaneous assessment of velocity by Doppler ultrasound and wall position is impossible, which hampers an accurate flow assessment.

As described in part A of this two-part manuscript (Beulen et al. 2010) ultrasonic perpendicular velocimetry (UPV) enables simultaneous assessment of axial velocity profile and vessel wall position. It was shown that for an accurate estimation of flow, no averaging is required, making a beat to beat analysis of pulsating flows possible. For flow estimation in curved geometries, Verkaik et al. (2009) introduced the cos θ method, which allows an accurate flow assessment based on integration of axial (asymmetrical) velocity profiles, assuming that the asymmetry in the velocity distribution is primarily caused by the local curvature of the vessel. The integration method is supported by the existing analytical approximations for steady and unsteady Newtonian flow in curved vessels (Dean 1927; Topakoglu 1967; Siggers and Waters 2005, 2008). Furthermore, a validation by means of CFD calculations has shown that this method is more accurate than the Poiseuille approximation for stationary Newtonian flow through weakly curved vessels (Verkaik et al. 2009).

The aim of this study is to test the applicability of the UPV assessment in combination with the cos θ method to assess axial velocity distribution and volume flow for steady and unsteady flow in curved vessels. In a phantom set-up, measurements of the axial velocity profile in planar curved vessels are taken by means of the UPV method. The flow conditions and vessel geometry are chosen to mimic flow in the common carotid artery (CCA). Results of the velocity profile measurements are compared with CFD calculations. The cos θ method is applied to estimate the volume flow from the asymmetric axial velocity profiles. The results are compared with the presently applied Poiseuille and Womersley approximations. Furthermore, a sensitivity analysis of the three integration methods to the exact orientation of the measured cross-sectional velocity profile of the artery is analysed by means of a CFD-based analysis.

2 Material and methods

2.1 Experimental set-up

In the experimental set-up (Fig. 1), a fluid, mimicking the acoustic and rheological properties of blood, was pumped

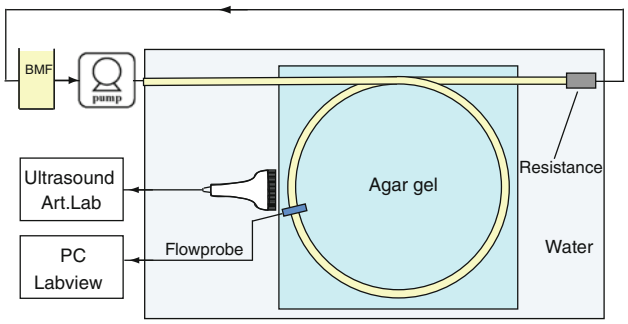

Fig. 1 Schematic overview of the experimental set-up

from a reservoir through a compliant tube, which mimics the blood vessel. A polyurethane tube (HemoLab, Eindhoven, The Netherlands) with a radius, a, of 4 mm and a wall thickness of 0.1 mm was applied to mimic the CCA. The polyurethane tube consisted of multiple straight and curved segments with a length of about 30 cm, produced with a spin coating method, which were smoothly glued together, resulting in a tube with a straight inlet and outlet section and a single curved centre section. Vessels with a curved section with a radius of curvature, R, of 20 cm and 40 cm were produced. This corresponds to a curvature ratio, $\delta = a/R$, of 0.01 and 0.02, respectively.

The phantom vessel was fully submerged in a water-filled reservoir to prevent the vessel to deform under influence of gravity. The curved section was positioned in a horizontal plane to prevent influence of gravity on the flow. Additionally, the water acted as a conductor of sound. The tube was terminated by a resistance, from which the fluid flowed back to the reservoir. For the terminal impedance, a Windkessel model was applied. The viscous dissipation in the distal vessel, R_s, and the viscous dissipation in the distal capillary bed, R_p, were modelled by local narrowing, and the compliance of the arterial system, C, was modelled by an air-chamber.

The flow was generated by combining a stationary pump and a servo-actuator operated piston pump (indicated in Fig. 1 by a single symbol). The stationary pump (Pacific Scientific, IL, USA) was manually set to a specific flow rate, whereas the trajectory of the piston pump (home developed) was computer controlled using LabView software (National Instruments, Austin, TX, USA).

To ensure a developed velocity distribution at the measurement site, the ultrasound probe was positioned at 270° from the inlet of the curve. The ultrasound probe was accurately positioned in the symmetry plane of the curve, perpendicular to the polyurethane tube, by means of a 3D manipulator, such that the mechanical focus of the probe was located at the centre of the vessel. To maximize the signal level, the electrical focus was set equal to the mechanical focus. At about 1 cm upstream

of the ultrasound probe, an ultrasonic flow probe (10PAA, Transonic, NY, USA) was positioned to measure the flow through the tube. The data from the flow probe measurements were acquired simultaneously with the data from the ultrasound scanner using a common trigger signal generated by a PC using the same LabVIEW data acquisition software.

For a description of the blood mimicking fluid (BMF), data acquisition and data processing, the reader is referred to Part A, Beulen et al. (2010).

2.2 Velocity measurements

2.2.1 *Stationary flow*

The stationary flow was generated with a constant head system positioned between the stationary pump and the inlet of the phantom vessel to attenuate possible flow oscillations caused by the stationary pump. By varying the resistance at the outlet of the phantom vessel, stationary flow rates varying from 0.15 to 1.15 l min^{-1} were generated, which corresponded to $50 < Re < 520$, in which the Reynolds number, Re, is defined as:

$$Re = \frac{2a\bar{v}\rho}{\eta(\dot{\gamma}_{\text{char}})}, \tag{1}$$

where $\bar{v}$ is the average axial velocity and ρ the BMF density. The effect of the non-Newtonian properties of the BMF was taken into account by incorporating the viscosity at the characteristic shear rate: $\eta = \dot{\eta}(\gamma_{\text{char}})$. The characteristic shear rate (Gijsen et al. 1999) was defined here as

$$\dot{\gamma}_{\text{char}} = \frac{2Q}{\pi a^3}, \tag{2}$$

in which Q is flow through the vessel and a, the radius of the vessel. Flow in curved geometries is characterized by the Dean number:

$$D = 4Re\sqrt{2\delta}, \tag{3}$$

in which Re is the Reynolds number and δ the curvature ratio. The flow in the tube with $\delta = 0.01$ was characterized by a Dean number $30 < D < 300$, the tube with $\delta = 0.02$, by $50 < D < 400$. Volume flow rates were measured by means of the Transonic flow probe, which was calibrated before each measurement using a stopwatch and a measuring beaker to collect steady flow. For each flow rate, an ultrasound measurement was taken. The RF data were filtered as described in part A, subsequently the UPV method was applied. A median filter with a temporal and spatial window size of respectively, $4 \cdot 10^{-3}$ s and $6.9 \cdot 10^{-5}$ m, was applied to remove outliers.

2.2.2 *Unsteady flow*

For the unsteady flow measurements, a pulsatile flow waveform (see Fig. 7) with a cycle time of 1 s, a mean of 0.7 l min^{-1} and a peak flow of about 1.6 l min^{-1} was generated by superimposing a flow pulse of the piston pump on a stationary flow component generated by the stationary pump. The resistance at the outlet was set high enough to prevent collapse of the vessel and low enough to induce low pressures, leading to negligibly small vessel wall motion and deformation. The stationary flow measurement was taken using the $\delta = 0.02$ geometry. To circumvent too large displacements of the tube due to the pulsatile pressure wave, the curved section of the vessel was fixed in space by placing the tube in an agar gel (1 wt% agar in water).

The generated flow waveform corresponded to physiologically relevant average and peak Reynolds numbers, equal to 300 and 900 respectively (Ku 1983). For the flow in the curved section, this corresponded to an average and peak Dean number, equal to 240 and 720, respectively. For the calculation of the Womersley parameter, $\alpha = a\sqrt{\omega\rho/\eta}$, it was assumed that $\eta = \eta(\dot{\bar{\gamma}}_{\text{char}}) = \eta(\frac{2\bar{Q}}{\pi a^3}) \approx 5 \cdot 10^{-3}$ $\text{kgm}^{-1}\text{s}^{-1}$. For the first harmonic, the Womersley parameter was found to be 4.5.

Using LabVIEW, the piston pump was programmed to generate 30 beats. Simultaneously, the flow was measured and a trigger signal was generated. During these 30 beats, 3.8 s of fast B-mode RF data were obtained for offline processing. The trigger signal was used to synchronize the flow measurement with the RF data. The RF data were filtered as described in part A. A median filter with a temporal and spatial window size of respectively, $4 \cdot 10^{-3}$ s and $6.9 \cdot 10^{-5}$ m, was applied to remove outliers. A low pass, zero-phase Butterworth filter with a cut-off frequency of 40 Hz was applied to suppress high frequency noise.

2.2.3 *CFD*

The UPV-based velocity estimation in curved geometries was validated by comparing the velocity profile measurements to CFD computations of the velocity profile. A finite-element CFD model of a rigid walled curved vessel (Beulen et al. 2009; van de Vosse et al. 2003) was applied to calculate the time-dependent fully developed velocity distribution across the vessel. The shear rate dependency of the viscosity was incorporated by implementing the Carreau-Yasuda model. For the boundary conditions, at the inlet, the flow as assessed in the experiments was prescribed. At the walls, the no-slip boundary condition was applied.

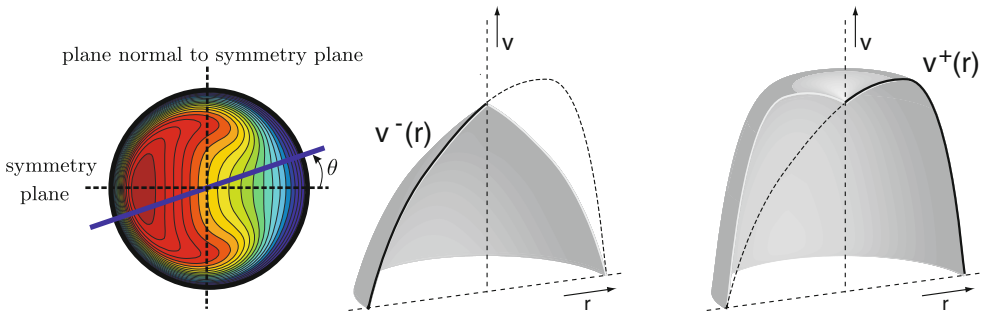

Fig. 2 Velocity profile in a curved tube indicating the integration angle θ (*left*). The beam direction was in the symmetry plane. Schematic explanation of the integration method (*right*): the measured axial velocity profile is divided into two equal parts at the centreline, $v^-(r)$ (*left*) and $v^+(r)$ (*right*). Each part is integrated over half the surface of the tube as if it were an axi-symmetric profile. The volume flow is approximated by summation of both contributions

2.3 Flow estimation

Volume flow was estimated from the measured axial velocity profiles by application of the cos θ method (Verkaik et al. 2009) and the Poiseuille and Womersley approximations. When a steady fluid flows through a curved tube, the maximum velocity is shifted towards the outside of the curvature, for a not too low flow rate (Fig. 2). This axial velocity profile is asymmetric along the centreline and can in first order be described as a correction to Poiseuille flow taking the form $f(r)\cos\theta$ for some function f (Siggers and Waters 2005). Because of the cosine function, only two points at the same distance r from the centreline are needed to determine the averaged value at a certain r. Therefore, a single line measurement along or nearly along the centreline is sufficient to make an accurate flow estimation. For the cos θ method, this was done by splitting the measured flow profile into two equal parts at the centreline, $v^+(r)$ and $v^-(r)$. Each part of the profile was integrated over half of the surface of the tube, based on the measured radius, as if it were an axi-symmetric profile (Fig. 2). The volume flow was approximated by summation of both contributions:

$$Q = \pi \int_0^a v^+(r) r dr + \pi \int_0^a v^-(r) r dr. \tag{4}$$

For Doppler velocity measurements, the exact position of the vessel walls and thus the position of the centre of the vessel are not known. For that reason, it is often assumed that the centreline velocity is equal to the maximum velocity measured over the cross section of the artery (Fraser et al. 2008). Accordingly, for the Poiseuille approximation, the measured velocity profile was approximated by a parabolic velocity profile with a maximum velocity equal to the measured maximum velocity. For the Womersley approximation, the inverse Womersley method (Cezeaux and Grondelle 1997) was applied to determine the flow rate from the measured maximum velocity. All three flow approximations were compared to the flow as assessed directly during the measurement.

2.4 Sensitivity analysis

For application of the flow approximation methods, it is frequently assumed that the acquired velocity distribution is obtained by measuring exactly through the centre of the vessel. However, in clinical practice, the exact orientation of the ultrasound beam, with respect to the cross section of the vessel, is not known and varies for each measurement. Depending on the shape of the velocity distribution and the approximation method applied, these uncertainties in positioning can result in significant misestimates in the flow deduced. In order to obtain an estimate of these deviations, the Poiseuille, Womersley and cos θ flow approximation methods were applied to CFD-derived velocity profiles. Contrary to an experimental investigation into the sensitivity, a CFD-based analysis allows to eliminate the influence of measurement errors in the velocity profile and probe positioning on the flow approximations and thus allows to solely focus on the performance of the approximation methods. At the inlet of the CFD model, the flow, as assessed in the unsteady flow experiment, was prescribed, at the walls, and the no-slip boundary condition was applied. It is assumed that the velocity profile is measured over a line oriented at an angle Φ with respect to the symmetry plane ($\theta = 0$) at a distance d from the centre of the cross section, perpendicularly positioned to the centreline of the vessel (Fig. 3). In this analysis, the cross section of the ultrasound beam is assumed to be constant and negligibly small.

The velocity profile was determined for $0 \leq \Phi \leq 2\pi$, with steps of $\pi/18$, and $0 \leq d \leq a/2$, with steps of $a/36$. For each combination of Φ and d, the apparent velocity profile was divided into two equal parts at the apparent centreline. Subsequently, the cos θ method was applied to determine the flow. Furthermore, the apparent maximum velocity was applied as an input for the Poiseuille and Womersley-based

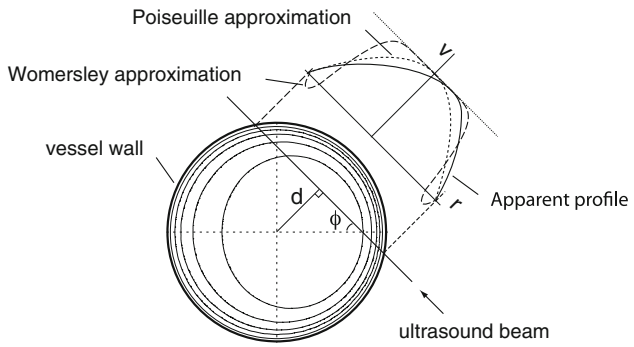

Fig. 3 Schematic overview showing the apparent velocity profile (input for the cos θ approximation) and the Poiseuile and Womersley approximations (based on the apparent maximum velocity) for an axial velocity assessment for which the ultrasound beam crosses the vessel at an angle Φ and a distance d, perpendicularly to the centreline

approximations. After applying a low pass, zero-phase Butterworth filter with a cut-off frequency of 40 Hz, the resulting flow waveforms were analysed by comparing the minimum, maximum and mean flow, pulsatility index and rise time to the corresponding properties of the prescribed flow waveform (Leguy et al. 2008). The pulsatility index was defined as the ratio of the difference between maximum and minimum flow and the time averaged flow. The rise time was defined as the time difference between the time-point with the maximum second derivative and the time-point with the maximum flow value. For the analysis, it was assumed that differences less than 10% between properties derived from the reference flow and integration-based flow waveform were adequate for in-vivo application.

3 Results

3.1 Stationary flow

A comparison between the mean velocity profiles for the ultrasound measurement and the CFD solution of the velocity profile is presented in Fig. 4. The results were non-dimensionalized by the radius, a, of the vessel. The ultrasound transducer was located at $r/a \approx -5$.

The measured velocity profiles agree quite well with the calculated velocity profiles. The root mean square value of the deviation between the measured and calculated velocity profiles is on average $1.7 \cdot 10^{-2}$ ms^{-1} for the measurements taken in the $\delta = 0.01$ geometry and $2.4 \cdot 10^{-2}$ ms^{-1} for the measurements taken in the $\delta = 0.02$ geometry. For the $\delta = 0.01$ geometry, the shift of the maximum velocity towards the outside of the bend appears to be less pronounced for the measured profiles than for the calculated profiles.

The volume flow is estimated from the measured asymmetric axial velocity profiles by means of the cos θ and the Poiseuille flow estimation method. A comparison of the integration-based flow estimates and the reference flow measurement by the flow probe for both the $\delta = 0.01$ and $\delta = 0.02$ geometry is presented in Fig. 5.

A linear fit shows that for the $\delta = 0.01$ curved vessel, the ratio between the cos θ-based flow estimate and direct flow measurement equals 0.97 ± 0.03, with a constant flow underestimation of -0.03 ± 0.03 l min^{-1}. For the $\delta = 0.02$ curved vessel, the ratio between the cos θ-based flow estimate and direct flow measurement equals 0.88 ± 0.06, with a constant flow underestimation of -0.01 ± 0.06 l min^{-1}. The CFD-based flow estimates show that especially at high Dean numbers and δ, the cos θ-integration method slightly underestimates the flow (about 5% for $q_{ref} \approx 1.1$ lmin^{-1}). At low flow rates, the deviation is negligible. At the lowest flow rates, the deviations found for the Poiseuille approximation are comparable to the deviations found for the cos θ method. However, for the Poiseuille approximation, these deviations increase to 20% for the high flow rates ($q_{ref} \approx 1.1$ lmin^{-1}).

3.2 Unsteady flow

A comparison between the instantaneous velocity profile measurements and the CFD solution of the velocity profiles

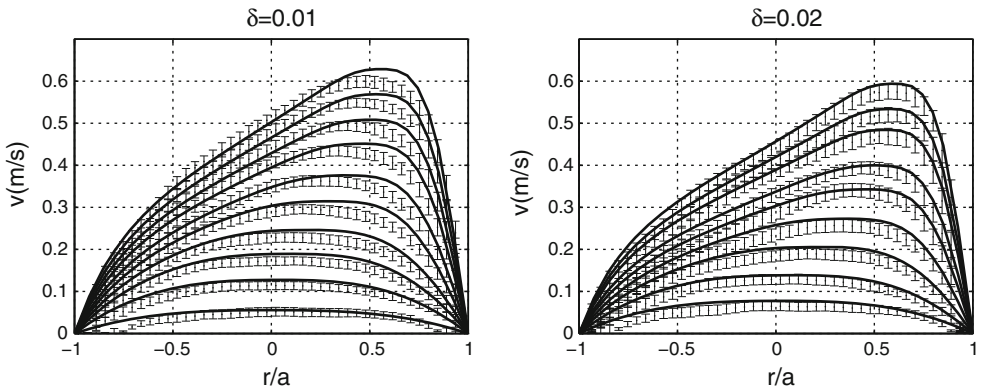

Fig. 4 Comparison of the ultrasound measurement (·) and the CFD velocity profile (−) for both the $\delta = 0.01$ and $\delta = 0.02$ geometry

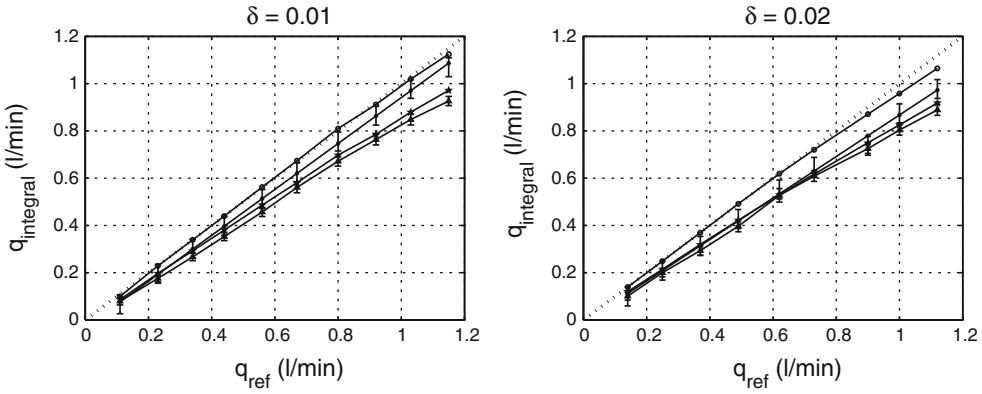

Fig. 5 Comparison of the flow estimation based on the cos θ (asterisks) and the Poiseuille method (open triangle) to the reference flow measurement for both the $\delta = 0.01$ and $\delta = 0.02$ geometry. Additionally, the flow is determined from the CFD-calculated velocity profiles using the cos θ (open circles) and the Poiseuille-method (star)

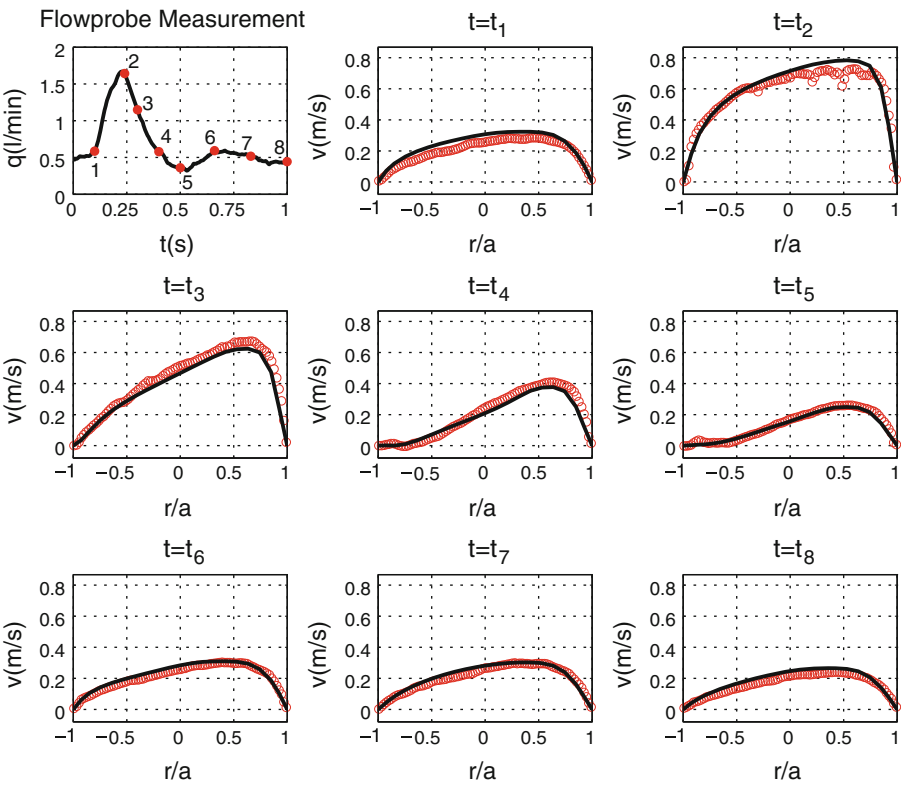

Fig. 6 Comparison of the ultrasound measurement and the calculated velocity profile (open circles) ultrasound measurement; – , CFD calculation)

is presented in Fig. 6. The velocity profiles are shown for eight distinct phases in the period. The results are non-dimensionalized by the radius, a, of the vessel. Again, the ultrasound transducer was located at $r/a \approx -5$.

Overall, the measurements agree very well with the calculated profiles, although some deviations occur at peak systole. The volume flow is estimated from the measured asymmetric axial velocity profiles by means of the cos θ model, the Poiseuille and Womersley approximations (Fig. 7). For the cos θ model, the grey zone indicates the standard deviation of the calculated flow rates.

The cos θ-based flow approximation agrees well with the reference flow as assessed using the flow probe, although some deviation occurs in the systolic peak. The Poiseuille and Womersley-based flow approximations clearly underestimate the flow, especially at peak systole.

3.3 Sensitivity analysis

The results of the comparison of the minimum, maximum and mean flow and the pulsatility index between reference flow waveform and integration-based flow waveform (Figs. 8, 9, 10) show the absolute percentual deviation

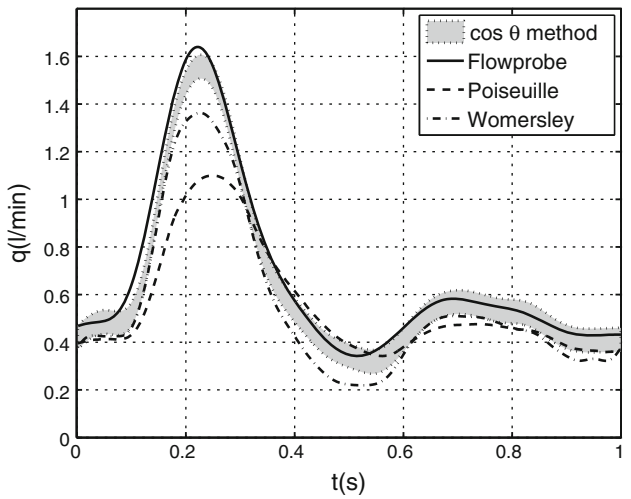

Fig. 7 Comparison between the flow probe measurement and the cos θ, Poiseuille and Womersley-based flow approximations. For the cos θ method, the *grey zone* indicates the standard deviation of the calculated flow rates

between reference and integration-based flow waveform for the aforementioned properties for different combination of angle, Φ, and offset, d. Regions with an absolute deviation above 10% are shaded.

The contour plots in Fig. 8 indicate that for the cos θ method, Q_{min}, Q_{mean} and the pulsatility index can be assessed with an estimation error of less than 10% for the major part of the (Φ, d)-space. However, the estimation of the maximum flow, Q_{max}, is found to be more sensitive for increasing d: for $d > a/10$, the deviation is already higher than 10%.

The contour plots presented in Figs. 9 and 10 show that both the Poiseuille and Womersley approximations can only be applied to adequately assess the minimum flow. For the maximum and mean flow and the pulsatility index, deviations between reference flow and integration-based flow are above 10% for the major part of the (Φ, d)-space. For the rise time, it is found that for the cos θ method, the mean deviation is 4% (max 8%) compared to respectively 1% (max 8%) and 6% (max 15%) for the Poiseuille and Womersley approximations with respect to the reference flow.

4 Discussion

For the stationary flow measurements, the shift of the maximum velocity towards the outside of the bend appears to be less pronounced for the measured profiles than for the

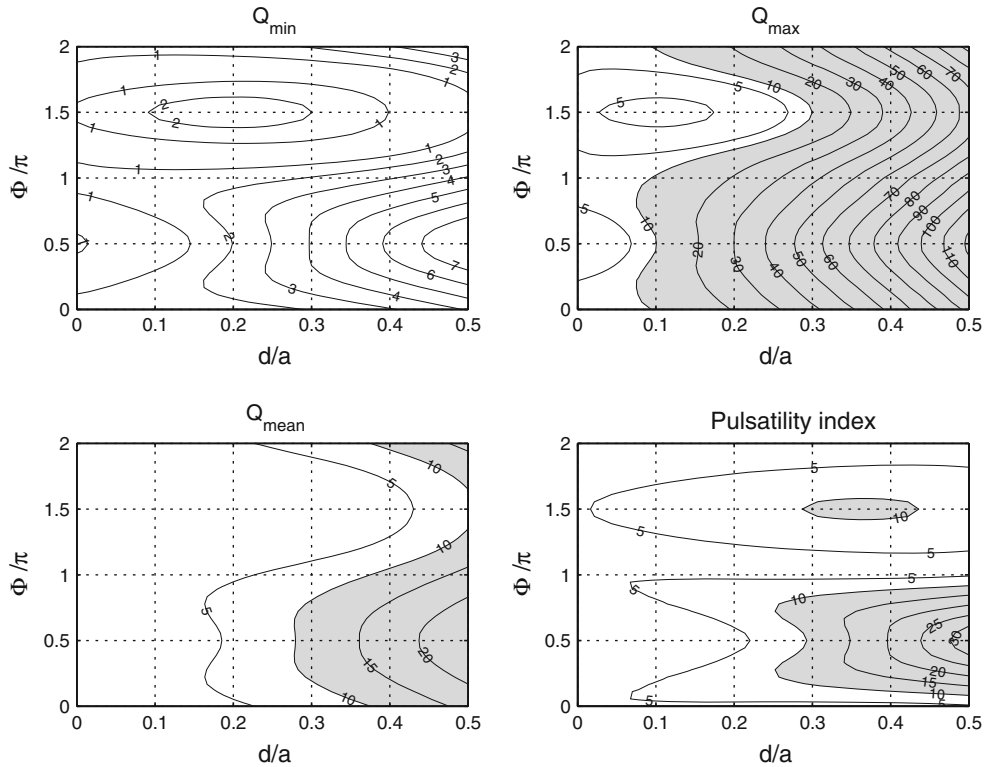

Fig. 8 Absolute deviation between the reference flow and the cos θ-based flow estimate for offset d and angle Φ. Deviations are expressed in percentages, regions with deviations larger than 10% are *shaded*

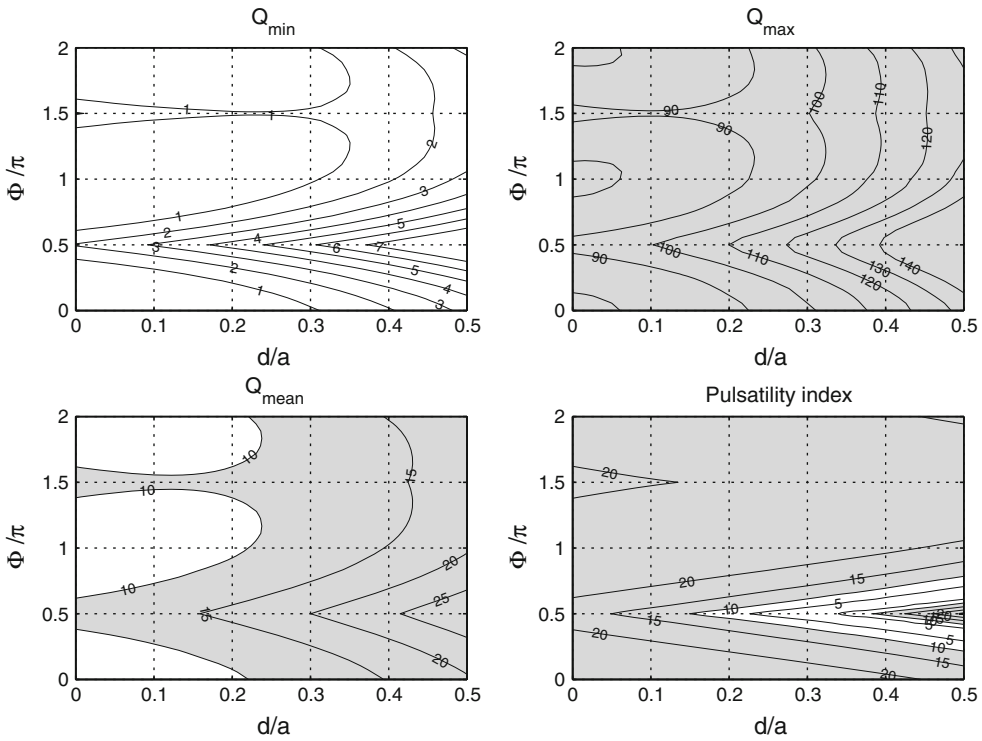

Fig. 9 Absolute deviation between the reference flow and Poiseuille-based flow estimate for offset d and angle Φ. Deviations are expressed in percentages, regions with deviations larger than 10% are *shaded*

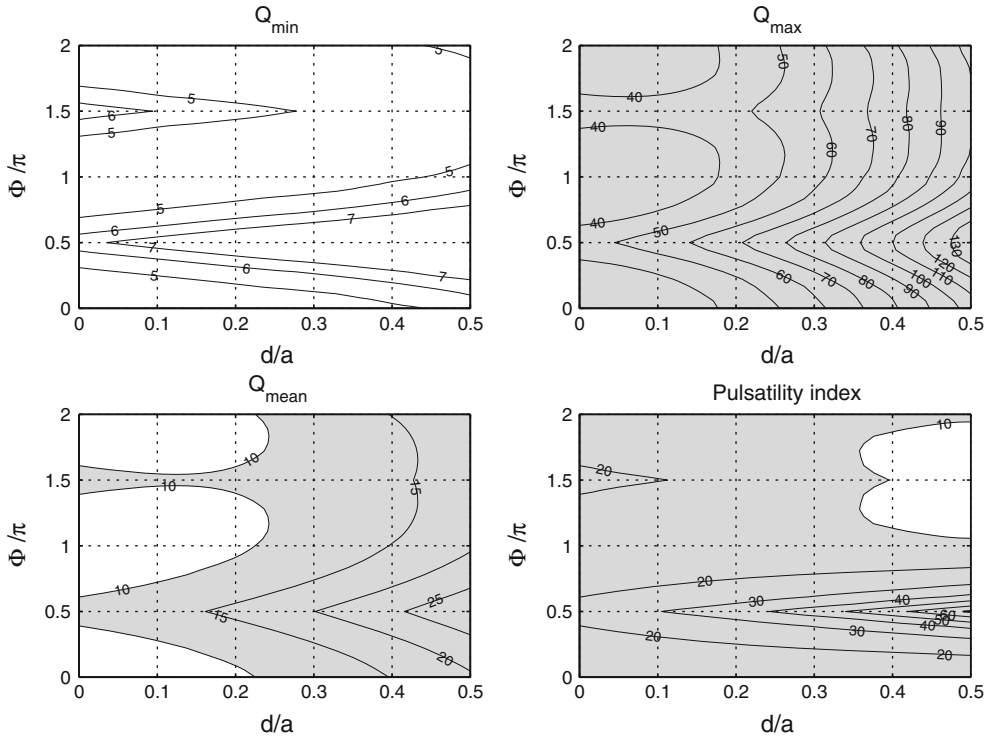

Fig. 10 Absolute deviation between the reference flow and Womersley-based flow estimate for offset d and angle Φ. Deviations are expressed in percentages, regions with deviations larger than 10% are *shaded*

calculated profiles. This deviation can be caused by the fact that the flow is not able to develop fully in the $\delta = 0.01$ geometry. It is difficult to position the curved sections of the vessel exactly in a horizontal plane, especially for the $\delta = 0.01$ geometry. Small vertical deviations from the horizontal plane can already result in local vertical

deviations which are in the same order as the curvature of the vessel. This prevents full flow development and can cause deviations from the CFD-calculated profiles. Additionally, for this weakly curved geometry, the measurement location might be not far enough from the entrance of the curved section to observe fully developed flow.

Overall, the deviations found between calculated and measured velocity profiles are comparable to the deviations found between calculated and measured velocity profiles in straight geometries (Beulen et al. 2010). Both for the $\delta = 0.01$ and $\delta = 0.02$ geometry, the deviation between the velocity profile measurements and calculated velocity profile increases in the near-wall region, $0.9 < |r|/a < 1.0$ and especially near the anterior wall ($r/a = -1$), probably due to the fact that the signal of the wall dominates the scattering signal in this region. Additionally, the high spatial velocity gradients can cause a decrease in accuracy of the velocity estimation.

For the measurements taken in the $\delta = 0.01$ geometry, the cos θ method proves to be quite accurate, with an average deviation of 3% with respect to the reference flow. For the measurements taken in the $\delta = 0.02$ geometry, this deviation increases to 12%. Deviations found between cos θ approximation and reference flow are comparable to the deviations reported by Verkaik et al. (2009) for Newtonian flow. The cos θ method is found to provide a much more accurate flow estimate than the Poiseuille approximation, especially for high flow rates (increasing Dean number) and increasing δ. This is to be expected, since the Poiseuille method offers a bad approximation for the flattened velocity profiles that occur for shear thinning fluids.

The analysis of the velocity profiles calculated by the CFD model has shown that the maximum deviation with respect to the reference flow, induced by the cos θ method, is about 5% for the examined flow rates. The larger deviation found in the measurements (12% for the $\delta = 0.02$ geometry) can be caused by errors in the measured axial velocity profile. This can be expected from the cross-correlation algorithm since for each data window, the average velocity is determined, and in the case of large radial velocity gradients, this can result in an underestimate of the velocity. Furthermore, close to the wall, the velocity profiles are distorted by the presence of the wall, also causing an underestimation of the velocity and thus an underestimation of the flow. Additionally, transverse velocity components, such as secondary velocity components that especially occur in curved vessels, can have an influence on the performance of the cross correlation-based velocity estimate.

For the unsteady flow measurements, the comparison between the velocity profile measurements and CFD computations shows that the cross correlation-based ultrasonic perpendicular velocimetry is able to cope with the relatively high temporal and spatial velocity gradients which occur in unsteady flow in curved vessels, allowing an accurate assessment of axial velocity distribution for unsteady flow in curved vessels. No beat to beat averaging is required to acquire usable velocity profiles. In the systolic peak, the velocity is slightly underestimated. It appears as if a cut-off for the maximum velocity occurs. This is probably caused by the fact that the displacement between two successive fast B-mode frames is too large. According to the one-quarter rule (Keane and Adrian 1992), the maximum axial displacement of particles in two successive frames is $W_{\mathrm{FOV}}/4$, in which W_{FOV} is the width of the field of view. For ultrasound cross correlation-based measurements (Liu et al. 2008), this results in a maximum axial velocity equal to:

$$v_{\max} \approx \frac{fW_{\mathrm{FOV}}}{4}. \tag{5}$$

For the ultrasound system employed in this research, f is equal to 730 Hz, resulting in $v_{\max} \approx 0.8\,\mathrm{ms}^{-1}$, which corresponds with a pixel displacement of three pixels and is about equal to the cut-off value found in the velocity measurements. The only possibility to increase the maximum measurable velocity, without decreasing the axial resolution (increasing W_{FOV}), is to increase the frame rate f. Considering the rapid development of ultrasound systems, it is to be expected that in near future ultrasound systems with increased frame rate will allow the assessment of higher maximum velocities.

Although the cos θ method was derived for flow estimation for stationary Newtonian flow through weakly curved vessels, it is found that this method is also successfully applicable to non-Newtonian flow for physiologically relevant flow and geometries. The average deviation between the cos θ-integration-based flow estimate and the reference flow is about 5% (max about 20%), compared to an average deviation of 20% (max about 40%) for both the Poiseuille and Womersley approximations.

For a successful clinical application, it is required that the flow estimation method is not too sensitive to the exact orientation of the measured velocity profile with respect to the centreline of the cross section. The sensitivity analysis shows that the considered approximation methods can all be successfully applied to estimate the minimum flow rate with an error of less than 10%. However, only the cos θ method is able to estimate the maximum, minimum and mean flow rate and the pulsatility index with an estimation error of less than 10%.

For the cos θ-method, it was found that in order to obtain an error of less than 10% in minimum flow, mean flow and pulsatility index, the beam should be positioned at $d < a/4$. For the maximum flow estimate is found that the

exact positioning is more strict: for $d > a/10$, the deviation is already higher than 10%. An experienced ultrasound operator should be able to locate the centre of a vessel within a 10% accuracy by finding the maximum possible vessel diameter and/or the maximum signal. This allows the cos θ-method to be applied for an accurate flow estimation. It should be noted that in practice, the ultrasound beam has a finite cross section. As a result, the estimated velocity always represents an average velocity over a certain measurement volume.

5 Conclusion

The UPV method has been applied for an accurate assessment of the axial velocity profile for both steady and unsteady non-Newtonian flow in weakly curved vessels in a phantom set-up. A comparison between measurements and CFD calculations of the velocity profile shows that the UPV-model allows an accurate assessment of the axial velocity distribution. The deviation between the time averaged ultrasound velocity profile measurement and the CFD solution is on average about 2 cms^{-1}. For flow estimation, the cos θ method, Poiseuille and Womersley approximations have been applied to the measured velocity profiles. For stationary flow, the maximum deviation of the cos θ method derived flow rate compared to the reference flow is 12%, whereas the Poiseuille approximation results in deviations up to 20%. For unsteady flow, the average error between the cos θ integration-based flow estimate and reference flow is about 5%, compared to an average deviation of 20% for both the Poiseuille and Womersley approximations.

A CFD-based comparison of the Poiseuille, Womersley and cos θ-integration methods indicates the Poiseuille and Womersley methods can only be applied to accurately assess minimum flow (error <10%). The cos θ method, however, is found to allow accurate (error <10%) assessment of the minimum, mean and maximum flow for velocity profiles assessed at $d < a/10$ from the centreline, independent on the angle Φ. Overall, ultrasonic perpendicular velocimetry, combined with the cos θ-integration method, proves to be an accurate flow estimation method for flow in slightly curved arteries such as the CCA. Furthermore, the results show that an accurate flow estimation is feasible, independent on the orientation of the measured velocity profile with respect to the plane of symmetry, even when not exactly measured through the centreline of the vessel. The study shows that the ultrasonic perpendicular velocity assessment method combined with the cos θ method could be a valuable asset for accurate flow assessment in superficial arteries such as the brachial artery and the CCA.

Acknowledgments This work is part of and was supported by EUREKA project E!3399 ART.MED, IS042015

References

Beulen BWAMM, Rutten MCM, van de Vosse FN (2009) Fluid structure interaction in distensible vessels: a time periodic coupling. J Fluids Struct. doi:10.1016/j.jfluidstructs.2009.03.002

Beulen BWAMM, Bijnens N, Rutten MCM, Brands PJ, van de Vosse FN (2010) Perpendicular ultrasound velocity measurements by cross correlation of RF data. Part A: validation in a straight tube. Exp Fluids. doi:10.1007/s00348-010-0865-5

Brands PJ, Willigers JM, Ledoux LAF, Reneman RS, Hoeks APG (1998) A noninvasive method to estimate pulse wave velocity in arteries locally by means of ultrasound. Ultrasound Med Biol 24(9):1325–1335

Brands PJ, Hoeks APG, Willigers JM, Willekes C, Reneman RS (1999) An integrated system for the non-invasive assessment of vessel wall and hemodynamic properties of large arteries by means of ultrasound. Eur J Ultrasound 9:257–266

Caro C, Fitzgerald G, Schroter R (1971) Atheroma and arterial wall shear: observation, correlation and proposal of shear dependent mass transfer mechanism for atherogenesis. Proc Royal Soc London Biol 117:109–159

Cezeaux JL, Grondelle A (1997) Accuracy of the inverse Womersley method for the calculation of hemodynamic variables. Ann Biomed Eng 25:536–546

Dean WR (1927) Note on the motion of fluid in a curved pipe. Phil Magazine J Sci 4(20):209–223

Douchette JW, Corl PD, Payne HM, Flynn E, Goto M, Nassi M, Segal J (1992) Validation of a Doppler guide wire for intravascular measurement of coronary artery flow velocity. Circulation 85:1899–1911

Fillinger MF, Schwartz RA (1993) Volumetric blood flow measurements with color Doppler ultrasonography: the importance of visual clues. J Ultrasound Med 3:123–130

Fraser KH, Meagher S, R BJ, Easson WJ, Hoskins PR (2008) Characterization of an abdominal aortic velocity waveform in patients with abdominal aortic aneurysm. Ultrasound Med Biol 34(1):73

Fung YC (1993) Biomechanics: mechanical properties of living tissue. Springer, Berlin

Gijsen FJH, van de Vosse FN, Janssen JD (1999) Influence of the non-Newtonian properties of blood on the flow in large arteries: unsteady flow in a 90 degree curved tube. J Biomech 32(7):705–713

Gill RW (1985) Measurement of blood flow by ultrasound: accuracy and sources of error. Ultrasound Med Biol 11:625–641

Keane RD, Adrian RJ (1992) Optimization of particle image velocimeters: 1. double pulsed systems. Meas Sci Technol 1:1202–1215

Krams R, Bambi G, Guidi F, Helderman F, van der Steen AFW, Tortoli P (2005) Effect of vessel curvature on Doppler derived velocity profiles and fluid flow. Ultrasound Med Biol 31(5):663–671

Ku DN (1983) Hemodynamics and atherogenesis at the human carotid bifurcation. Ph.D. thesis, Georgia Institute of Technology

Laurent S, Cockcroft L, Van Bortel L, Boutouyrie P, Giannattasio C, Hayoz D, Pannier B, Vlachopolous C, Wilkinson I, Struijker-Boudier H (2006) Expert consensus document on arterial stiffness: methodological issues and clinical applications. Eur Heart J 27:2588–2605

Leguy CAD, Bosboom EMH, Hoeks APG, van de Vosse FN (2008) Assessment of blood volume flow in slightly curved arteries from a single velocity profile. J Biomech. doi:10.1016/j.jbiomech.2009.04.032

Liu L, Zheng H, Williams L, Zhang F, Wang R, Hertzberg J, Shandas R (2008) Development of a custom-designed echo particle image velocimetry system for multi-component hemodynamic measurements: system characterization and initial experimental results. Phys Med Biol 53:1397–1412

Siggers J, Waters S (2005) Steady flows in pipes with finite curvature. Physics of fluids 17(077102)

Siggers J, Waters S (2008) Unsteady flows in pipes with finite curvature. J Fluid Mech 600:133–165

Topakoglu HC (1967) Laminar flows of an incompressible viscour fluid in curved pipes. J Math Mech 16(12):1321–1337

Verkaik AC, Beulen BWAMM, Rutten MCM, Bogaerds ACB, van de Vosse FN (2009) Estimation of volume flow in curved tubes based on analytical and computational analysis of axial velocity profiles. Phys Fluids 21(2):023,602–1/13

van de Vosse FN, de Hart J, van Oijen CHGA, Bessems D, Gunther TWM, Segal A, Wolters BJBM, Stijnen JMA, Baaijens FPT (2003) Finite-element-based computational methods for cardiovascular fluid-structure interaction. J Eng Math 47(3–4):335–368